

Calorimetric study of nematic prewetting

XUEWU LIU, D. W. ALLENDER and D. FINOTELLO

Department of Physics, Kent State University - Kent, OH 44242-0001, USA

(received 12 November 2001; accepted in final form 20 June 2002)

PACS. 61.30.Gd – Orientational order of liquid crystals; electric and magnetic field effects on order.

PACS. 64.70.Md – Transitions in liquid crystals.

PACS. 68.08.Bc – Wetting.

Abstract. – We report specific-heat measurements for a series of liquid crystals imbedded in a porous cylindrical geometry. Above the nematic-to-isotropic transition and dependent on nematic width (or chain length), the specific heat shows a small peak. In analogy to known ellipsometry results, the peak is believed to be the signature of a nematic prewetting transition.

The behavior of liquid crystals (LC) at interfaces has been extensively researched due to the fundamental phenomena present and the possible impact on technological applications. Typical studies have determined the orientational anchoring and/or wetting behavior of LC at solid substrates or at the air interface [1–3]. Using ellipsometry on planar LC films, Lucht *et al.* [4–6] investigated the wetting behavior at the free surface, above the nematic (or smectic-A) to isotropic phase transition for several LC series. Above the smectic-A-to-isotropic (AI) transition of non-polar compounds they observed either i) complete wetting, or ii) partial wetting with pretransitional increase of surface order, or iii) partial or non-wetting without any pretransitional increase. They reported the first observation of a prewetting transition in a LC system 0.3 K above the bulk nematic-to-isotropic (NI) transition for a 1 mm thick planar film formed from the $\overline{10.O.8}$ compound [5]. The nematic prewetting signature arose from a homeotropically aligned, 12 nm thick, orientationally ordered layer. Broadly, the study of wetting and prewetting transitions has grown enormously in recent years. A review by Bonn and Ross [7] summarizes experimental observations of wetting and prewetting, recaps some major theoretical predictions, and provides references to earlier review articles on the subject. The primary observations of prewetting transitions have been in superfluid helium and in binary mixtures [8]. Note that a calorimetry study for LC in a porous interconnected medium [9] showed two specific-heat peaks, one of which disappeared after long-term annealing; those results were not cast in a wetting language.

We report specific-heat studies as a function of temperature for members of the LC series $\overline{m.O.8}$ confined to the submicron pores of Anopore membranes. Our goal was to determine if wetting (prewetting) yielded a thermodynamic signature due to the onset of an increase in orientational order. We chose a confined system for the following reasons. If our experimental sample were in the same geometry as [4, 5], one would have to extract the contribution to the specific heat due to a few nanometers thick layer of LC out of a one millimeter thick

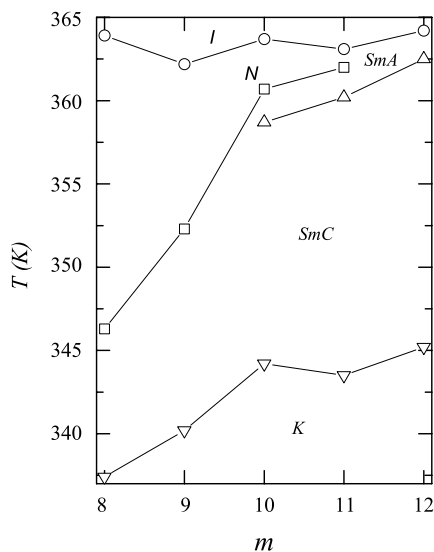


Fig. 1

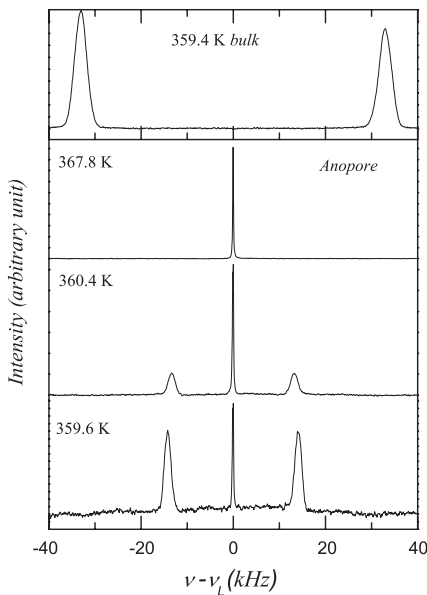


Fig. 2

Fig. 1 – Phase diagram for the bulk liquid crystal series $\overline{m}.O.\overline{8}$ as a function of chain length m .

Fig. 2 – DNMR spectra for bulk (top panel) and Anopore confined $\overline{10}.O.\overline{8}$ (bottom panels). The largest frequency separation in the confined sample is about one half that in bulk.

film; this would be difficult. Under confinement, the fraction of molecules in contact with the surfaces is large, yielding a resolvable signal as was shown by recent deuteron nuclear magnetic resonance (DNMR) studies of the orientational order of monolayer size LC films [10]. Anopore membranes were chosen due to their morphology and because, in previous specific-heat studies, cyanobiphenyls showed a discrete growth of the smectic phase at temperatures deep into the isotropic phase [2]. Because of its large pore size as compared to the molecular length, the Anopore confinement is known to affect the NI transition by a downshift in transition temperature and some rounding at the specific-heat maximum.

The confined molecular configuration was determined with DNMR; the specific heat was determined with ac calorimetry. For nematic $\overline{m}.O.\overline{8}$ members, there is a small specific-heat peak at a temperature T_{PN} above the main specific-heat peak at T_{NI} . The location of T_{PN} depends on the chain length, thus, on nematic width. The small peak is not detected if the pores are first coated with a chemical surfactant, either lecithin or an aliphatic acid, before imbedding the LC. If the LC lacks the nematic phase, a smectic wetting of the surface is also found. The small specific-heat peak is related to nematic prewetting of the solid interface. Phase shift results suggest that a surface transition occurs.

Anopore membranes [2, 10] consist of a high-purity Al_2O_3 matrix with $0.2\ \mu m$ diameter cylindrical pores through their $60\ \mu m$ thickness. Anopore membranes have many desirable features for confined studies: large porosity ($> 40\%$), high surface-to-volume ratio to maximize surface interaction, robust and chemically treatable surface, well-defined, and narrow pore size distribution. Using Anopore as the host, we studied $\overline{m}.O.\overline{8}$ for $m = 8 \rightarrow 12$. For reference, a phase diagram was obtained by differential scanning calorimetry for the bulk compounds, fig. 1. A low-temperature smectic-C (SmC) phase is always present above the crystal (K)

phase. The nematic width decreases with increasing chain length, vanishing for $m = 12$; the intermediate smectic-A (SmA) phase first appears for $m = 10$.

To verify that our experimental conditions resemble those of [4, 5], our most extensively studied LC sample, $\overline{10.O.8}$, was deuterated and DNMR spectral patterns were obtained. In fig. 2, we compare the confined spectra with the pores oriented parallel to the NMR 4.7 T external magnetic field, with that of the bulk material fully aligned by the NMR field [11]. The bulk pattern is a quadrupole splitting $\delta\nu$ (frequency separation between the two absorption peaks) of about 65 kHz. Such a frequency splitting characterizes the presence of an orientationally ordered phase; its size is proportional to the amount of order

$$\delta\nu = \delta\nu_0 Q \langle P_2 \rangle = \delta\nu_0 Q \left\langle \frac{1}{2} (3 \cos^2 \theta_B - 1) \right\rangle, \quad (1)$$

with $\delta\nu_0$ the maximum frequency splitting observable in a fully aligned bulk nematic sample, Q the scalar orientational order parameter, and θ_B the angle between the LC director and the NMR field. For bulk, $\theta_B = 0^\circ$ due to the magnetic-field-induced uniform alignment of the director along the field. In Anopore, with decreasing temperature, the spectrum evolves from a high temperature, sharp central peak typical of the isotropic phase, to a pair of peaks, the quadrupole splitting. The confined quadrupole splitting (bottom panel of fig. 2) at a comparable temperature is nearly one half that of bulk (top of fig. 2). The reduced splitting shows that the confined configuration is consistent with molecules aligned perpendicular to the field ($\theta_B = 90^\circ$ in eq. (1)), or perpendicular to the pore's axis [2, 10].

Since a prewetting signature would arise from an orientationally ordered surface layer, our initial expectation was to find a DNMR feature. Surface wetting may be manifest as an isotropic peak whose width increases cooling towards the transition, perhaps even showing a jump (in bulk, the width of the peak is temperature independent [3]). Here, due to the high temperature where the transition to the isotropic phase occurs and the temperature control in our magnet (± 0.1 K), there is only a small increase in the peak width, 2-3 times broader than in bulk.

The temperature control and resolution is threefold higher in the ac calorimeter than in the magnet [2]. The calorimeter has an internal time constant of about 1.26 s (0.79 Hz high-frequency roll-off) and an external time constant of 31.4 s (0.032 Hz low-frequency roll-off). The addendum heat capacity from the sapphire disk holder, thermometer and heater is 42 mJ/K at 303 K, increasing linearly with temperature at a rate of 0.286 mJ/K². The oscillating voltage frequency was maintained between 50 and 100 mHz and the induced temperature oscillations kept on the order of 3 mK while spacing data by 10–15 mK. The typical sample consisted of a single Anopore cut to a disk 9 mm in diameter containing 3 mg of LC completely filling the pores.

The calorimetric results in fig. 3 focus on the transition to the isotropic phase; all bulk phase transitions are also detected in the confined system but are not shown in fig. 3. For $\overline{8.O.8}$, of the widest nematic range, fig. 3a, there is a prominent specific-heat peak at the NI transition: pretransitional fluctuations on the nematic side, confinement-induced rounding near the peak's maximum, and a reasonably sharp decrease into the isotropic phase, typical features at the NI specific-heat peak. As m increases and the nematic width decreases, unlike bulk, an additional feature appears at a temperature above the confined T_{NI} . For $\overline{9.O.8}$, fig. 3b, the NI specific-heat peak splits near the maximum with a small peak developing on the isotropic side. In $\overline{10.O.8}$, the small peak shifts to a higher temperature in the isotropic phase (now resembling a bump); it is indicated in fig. 3 by T_{PN} [12]. The shift in temperature of this feature continues with increasing m for the next two members of the homologous series,

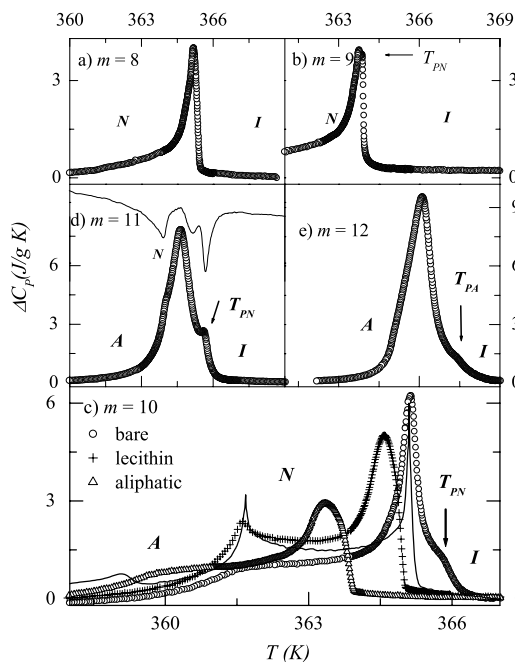


Fig. 3

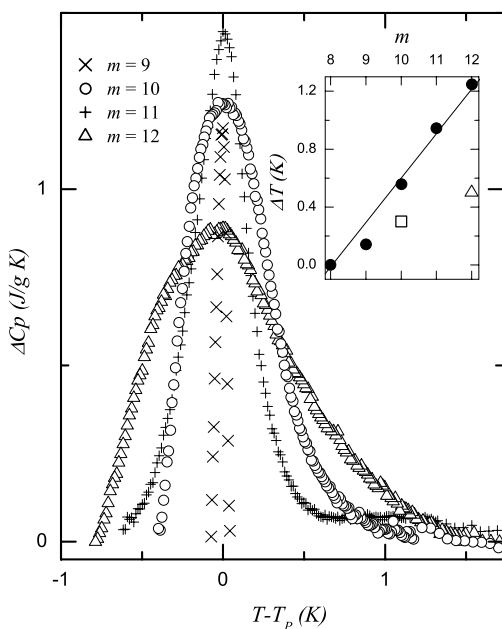


Fig. 4

Fig. 3 – Specific-heat results in Anopore. For $\overline{10.O.8}$, also included in (c) are bulk (solid line) and after surfactant coating of the pores. The prewetting signature is indicated by the arrows. For $\overline{11.O.8}$ (d), the phase shift temperature dependence plotted on an arbitrary scale is also shown (solid line).

Fig. 4 – Excess specific heat after arbitrary background subtraction. The asymmetric nature of the peak for $\overline{12.O.8}$ is suggestive of its different nature. Inset: temperature separation between the prewetting signature and the main transition peak as a function of m (solid circles). Also included are selected ellipsometry results from [4], the triangle for $\overline{10.O.8}$ and the square for $\overline{12.O.6}$. The straight solid line is a guide to the eye.

$\overline{11.O.8}$ (fig. 3d) and $\overline{12.O.8}$ (fig. 3e). Since the latter compound lacks a nematic phase, the wetting signature is thus identified by T_{PA} (see below). Finally, fig. 3c also shows the bulk result (solid line) with no additional features.

While the temperature location of a prewetting signature depends on anchoring energy (substrate dependent), the calorimetric prewetting feature is at a temperature comparable to the ellipsometry work. This is stressed in the inset to fig. 4 showing the separation between the prewetting peak temperature T_{PN} (or T_{PA}) and T_{NI} (or T_{AI}) as a function of chain length m . This dependence appears to be linear although its significance is not clear; it may be a result of a LC-dependent anchoring energy. Also seen in the inset to fig. 4 are ellipsometry results for two other LC compounds at an air interface. Thus, we interpret the specific-heat peak at $T_{PN} > T_{NI}$ as the thermodynamic signature of nematic prewetting.

That the signature is related to prewetting of the Anopore surfaces is seen by precoating its pores with a 2% solution of a surfactant: either lecithin or an aliphatic acid, before imbedding the LC material. Such concentration was chosen as it yields a uniform coating of the pores [3]. For cyanobiphenyls in Anopore these surfactants induce homeotropic anchoring conditions and increase the surface-LC interaction [3]. Specific-heat results for $\overline{10.O.8}$ in surfactant-coated

Anopore, fig. 3c, show that for both surfactants the NI peak is downshifted, round and broad; unlike the bare pore case, above T_{NI} there is only a bulk-like smooth decrease to the isotropic phase. This suggests that the surface interaction has increased beyond the critical point for the prewetting line [13]. Hence, the prewetting signature is only accessible over a narrow surface-LC interaction range, explaining the difficulties in observing it. Finally, in smectic $\overline{12.O.8}$, the specific heat also shows a feature on the high-temperature side. This is not unlike observations in smectic-A cyanobiphenyls [2]; this signature reflects that surface-induced (but now) layered orientational order is present.

Quantitatively, we assume a bulk-like decrease to the isotropic phase in the specific heat and use it as a “background”; this arbitrarily chosen background is subtracted from the measurement. The remaining or “excess” specific heat is associated with surface prewetting and is plotted as a function of temperature in fig. 4. For $m = 9$ to 11, the prewetting peak is reasonably symmetric and sharp; its height increases with increasing chain length. For $m = 12$, the peak is broader, asymmetric, and of smaller height, all characteristics that suggest its different nature. More importantly, by comparing the area under the prewetting peak with the total area under the complete T_{NI} peak, we can estimate the number of LC molecules yielding the prewetting transition. We find that for $m = 9$ to 11 chain length, 8 to 12% of the molecules are in the surface-induced ordered phase contributing to the prewetting signature. This corresponds to an orientationally ordered layer approximately 10 nm thick prewetting the pore’s walls. This agrees with the more accurate determination from ellipsometry of 12 nm at an air interface; given the roughness of our estimate, the agreement is remarkable.

Jerome’s review [14] provides connections to early experimental work; at that time, no prewetting transition had been observed near NI. Theory offers several possibilities for the transition, producing both the prewetting peak and the main NI peak, depending on the surface interaction and the structure of the confined nematic. In a confined nematic the spatial variations of the tensor order parameter can be split into: 1) changes in the direction of the principle axes, or directors, and 2) changes in the degree of orientational order, *i.e.*, the tensor eigenvalues. For homeotropic anchoring conditions (as here) at the surface and temperatures where the nematic phase occurs, DNMR for cyanobiphenyls in Nuclepore indicates that a planar polar director is expected [15]. Such a pattern has two defect lines of strength one-half on the cylindrical surface which are parallel to the cylinder axis. For cases with larger diameter pores, the configuration known as the escaped structure is likely [16]. A planar radial pattern [17] was also considered, but it always yielded a higher-energy state. Other studies [18,19] found that the core structure of the defect lines in the planar and/or radial structures should involve biaxial orientational order [10].

Surface transitions involving the LC orientational order but no changes in the direction of the directors have been studied for planar and spherical surfaces; cylindrical surfaces are expected to behave similarly. Sheng [13] first predicted a prewetting transition above T_{NI} due to homeotropic surface interaction at a planar wall. The uniaxial orientational order has a step-wise increase at the prewetting transition; this first-order transition is consistent with the observations by Lucht *et al.* [4–6]. For a surface where LC molecules lie randomly oriented in the surface plane, the prewetting transition involves a change from uniaxial to biaxial orientational order [20]. To develop a planar polar structure with biaxial defect cores is more involved than for planar surfaces and is likely to include director changes and changes in orientational order.

The theoretically expected phase diagram for surface transitions in LC systems is connected to the general picture of wetting phenomena [7]. It follows from the work of Nakanishi and Fisher [21] noting that it corresponds to a cut through their temperature–bulk field–surface field phase diagram by a plane defined by a linear relationship between temperature and bulk

field. Ideally, one would like to experimentally map out the prewetting line from its maximal first-order character at the juncture with the bulk NI coexistence line to the vanishing discontinuity at the prewetting critical point at the highest temperature above coexistence. However, the surface interaction strength is not a finely tunable experimental variable. We were able to probe different regions of the prewetting line only by changing the surface treatment or using different members of the LC series. Since ac calorimetry is not sensitive to latent heats, we are unable to observe the decrease of the first-order discontinuity as ΔT increases. Conversely, as the prewetting critical point is approached with increasing ΔT , the effect of pretransitional fluctuations increases yielding a broader peak, as seen in fig. 4. Thus, the increase of peak width with ΔT supports its identification as prewetting.

In our calorimeter at a phase transition there is a feature in the concurrently measured phase shift [22]. Typified by $\overline{11.O.8}$ in fig. 3d, the phase shift has a complex temperature dependence due to the several phase transitions present. Specifically, it shows a “dip” in the region of the prewetting signature, with the dip minimum at T_{PN} [23]. A feature in the phase shift further supports the fact that a transition occurs.

In short, analogous to the ellipsometry studies, our Anopore results can be understood in terms of a thermodynamic signature of nematic prewetting of the solid surface. The prewetting signature arises from a ~ 10 nm thick orientationally ordered layer at the surface.

* * *

We thank R. LUCHT for useful discussions, CH. BAHR for giving us the same compound used in his work, and V. SURENDRANATH for the LC compounds; research was supported by NSF ALCOM Grant No. 89-20147.

REFERENCES

- [1] VANDENBROUK F., VALIGNAT M. P. and CAZABAT A. M., *Phys. Rev. Lett.*, **82** (1999) 2693.
- [2] IANNACCHIONE G. S., MANG J. T., KUMAR S. and FINOTELLO D., *Phys. Rev. Lett.*, **73** (1994) 2708; IANNACCHIONE G. S. and FINOTELLO D., *Phys. Rev. E*, **50** (1994) 4780; *Phys. Rev. Lett.*, **69** (1992) 2094.
- [3] CRAWFORD G. P., ONDRIS-CRAWFORD R. J., ZUMER S. and DOANE J. W., *Phys. Rev. Lett.*, **70** (1993) 1838.
- [4] LUCHT R. and BAHR CH., *Phys. Rev. Lett.*, **78** (1997) 3487.
- [5] LUCHT R., BAHR CH., HEPPKE G. and GOODBY J. W., *J. Chem. Phys.*, **108** (1998) 3716.
- [6] LUCHT R., BAHR CH. and HEPPKE G., *Phys. Rev. E*, **62** (2000) 2324.
- [7] BONN D. and ROSS D., *Rep. Prog. Phys.*, **64** (2001) 1085.
- [8] Examples of prewetting transitions can be found in superfluid helium (TABOREK P. and RUTLEDGE J., *Phys. Rev. Lett.*, **68** (1992) 2184) and in binary mixtures (KELLAY H., BONN D. and MEUNIER J., *Phys. Rev. Lett.*, **71** (1993) 2607).
- [9] DADMUN M. D. and MUTHUKUMAR M., *J. Chem. Phys.*, **98** (1993) 4850.
- [10] ZALAR B., ZUMER S. and FINOTELLO D., *Phys. Rev. Lett.*, **84** (2000) 4866.
- [11] Since the magnetic coherence length is larger than the pore size, the confined configuration is surface induced.
- [12] We studied a $\overline{10.O.8}$ sample provided by Ch. Bahr used in his study [4]. The results are similar but the prewetting signature is less pronounced.
- [13] SHENG P., *Phys. Rev. A*, **26** (1982) 1610.
- [14] JEROME B., *Rep. Prog. Phys.*, **54** (1991) 391.
- [15] ALLENDER D. W., CRAWFORD G. P. and DOANE J. W., *Phys. Rev. Lett.*, **67** (1991) 1442.
- [16] CLADIS P. E. and KLEMAN M., *J. Phys. (Paris)*, **33** (1972) 591.

- [17] CRAWFORD G. P., ALLENDER D. W. and DOANE J. W., *Phys. Rev. E*, **45** (1992) 8693.
- [18] SLUCKIN T. J. and PONIEWIERSKI A., *Phys. Rev. Lett.*, **55** (1985) 2907.
- [19] KRALJ S., ZUMER S. and ALLENDER D. W., *Phys. Rev. A*, **43** (1991) 2943.
- [20] KOTHEKAR N., ALLENDER D. W. and HORNREICH R. M., *Phys. Rev. E*, **49** (1994) 2150; SEIDIN R., HORNREICH R. M. and ALLENDER D. W., *Phys. Rev. E*, **55** (1997) 4302.
- [21] NAKANISHI H. and FISHER M. E., *Phys. Rev. Lett.*, **49** (1982) 1565.
- [22] The induced temperature oscillations are out of phase with the sinusoidally applied heat. The phase shift contains information on the heat capacity and thermal conductivity of the sample mixed with thermal contributions from the addendum materials.
- [23] The phase shift for $\overline{12.O.8}$ (not plotted) shows a less pronounced peak in the neighborhood of the prewetting signature.